Sessarego and Wood *Renewables: Wind, Water, and Solar* (2015) 2:9
DOI 10.1186/s40807-015-0009-x

Renewables:
Wind, Water, and Solar
a SpringerOpen Journal

ORIGINAL RESEARCH PAPER Open Access

Multi-dimensional optimization of small wind turbine blades

Matias Sessarego[1,2] and David Wood[2*]

Abstract

This paper describes a computer method to allow the design of small wind turbine blades for the multiple objectives of rapid starting, efficient power extraction, low noise, and minimal mass. For the sake of brevity, only the first two and the last objectives are considered in this paper. The optimization aimed to study a range of blade materials, from traditional fibreglass through sustainable alternatives to rapid prototyping plastic. Because starting performance depends on blade inertia, there is a complex interaction between the material properties and the aerodynamics. Example blades of 1.1 m length were designed to match a permanent magnet generator with a rated power of 750 W at 550 rpm. The materials considered were (a) traditional E-glass and polyester resin; (b) flax and polyester resin; (c) a typical rapid prototyping plastic, ABS-M30; and (d) timber. Except for (d), hollow blades were used to reduce the rotor inertia to help minimize starting time. Two airfoils are considered: the 10% thick SG6043 which has excellent lift:drag performance at low Reynolds number and the SD7062 whose extra thickness (14%) has some structural advantages, particularly for the weaker material (c). All blade materials gave feasible designs with material (d) the only one that required a blade shell thickness greater than the specified minimum value of 1% of the blade chord. Generally, the blade chord and twist increased as starting was given greater importance. In all cases, the associated increase in blade inertia was outweighed by the larger aerodynamic torque. Materials (a), (b), and (d) were better suited to the SG6043 airfoil whereas ABS-M30 benefitted from the thicker SD7062 section.

Keywords: Small wind turbines; Blade design; Multi-dimensional optimization; Power; Starting performance

Background

Small wind turbines are under strong competitive pressure from photovoltaics (PV) which have decreased significantly in price over the past decade. A similar reduction in the manufacturing cost of small wind turbines is probably not achievable, but significant efforts can be made in this direction. For example, the recent increase in the use of monopole towers may well be reversed and the cheaper lattice tower gain renewed application (Adhikari et al. 2014a).

In addition, there are two aspects of small wind turbines that will remain attractive. The first is that remote renewable energy systems generally should use multiple resources, such as sun and wind, to provide the most cost-effective system despite any cost difference between the technologies (e.g. Kaldellis 2010). Second, most developing countries must import PV equipment, whereas there is scope for significant local manufacture of many wind turbine components, often using indigenous and sustainable materials, such as bamboo for the tower (Adhikari et al. 2014b) and timber or bio-composites and bio-resins for the blades (Peterson and Clausen 2004, Holmes et al. 2009, Astle et al. 2013, and Shah et al. 2013). In addition, the recent advent of rapid prototyping brings the promise of cheap manufacture of the complex three-dimensional blade shape and the potential to design blades for specific applications, such as rapidly starting blades for low-wind areas or especially quiet blades for building mounting.

In order to exploit these opportunities, the small wind turbine blade design must become increasingly multi-dimensional. Starting is often a critical issue for small blades as most do not have pitch adjustment. Recent two-dimensional optimizations considered starting and

* Correspondence: dhwood@ucalgary.ca
[2]Department of Mechanical and Manufacturing Engineering, University of Calgary, Calgary, AB, Canada
Full list of author information is available at the end of the article

power extraction (Wood 2011, Pourrajabian and Mirzaei 2014, and Shah et al. 2014). Clifton-Smith (2010) added noise. The common finding of these studies is that a multi-dimensional design is actually a trade-off. Typically, the most powerful blade is the slowest to start and Clifton-Smith (2010) found that for blades of nearly equal power extraction, the quietest blade was the slowest to start whereas the fastest starting blade was the noisiest.

Of the papers just cited, only Pourrajabian and Mirzaei (2014) considered structural optimization which is important for large-blade design partly because blade manufacturing cost correlates with blade weight (e.g. Sessarego et al. 2014). Structure is important for small blades in another way: starting depends on the aerodynamic torque generated by the blade shape and is improved by a low blade inertia, J_B, which depends on shape, material, and manufacturing technique. It is to be expected that including structure in small-blade optimization will introduce complex interactions between the objective functions. To fully exploit the possibilities of structural optimization, it is necessary to design hollow blades, whose shell thickness can be minimized to reduce J_B while remaining sufficiently strong. Examples of hollow composite small turbine blades are given in Clausen et al. (2013).

The aim of this paper is to explore multi-dimensional small wind turbine blade optimization including structure, by designing hollow blades using (a) traditional E-glass and polyester; (b) flax and polyester; (c) a strong, rapid prototyping material; and (d) solid blades using timber. The 1.1-m-long blades were designed to match a permanent magnet generator with a rated capacity of 750 W at 550 rpm and efficiency of 74%. Solid timber blades for this generator were designed in Chapter 7 of Wood (2011). The optimizations use the MATLAB code Small Wind-turbine Rotor Design Code (SWRDC) developed by the authors and available from them. The code combines the multi-objective problem in a single objective by using a scalarization function of all the objective functions, as explained below. Optimization is by a simple genetic algorithm.

Material (a) is typical of many current small blades. The use of flax rather than E-glass in material (b) is one way to reduce the environmental footprint of small blades (Shah et al. 2013). Timber, material (d), is commonly used for ultralight aircraft propellers and also may be environmentally preferable to material (a). Hoop pine is a native Australian tropical pine that grows well in plantation (Peterson and Clausen 2004) and has been used for many years for propeller manufacture[a]. It is possible that the advent of rapid prototyping or three-dimensional printing will revolutionize small-blade manufacture because it does not need expensive moulds and allows specific blade design for specific site conditions. For example, a windy site may not require rapidly starting blades, whereas a turbine to be installed next to a house may need to be extremely quiet. SWRDC is a very suitable tool to undertake the initial design of blades for different requirements. However, there is one major concern with rapid prototyping materials: an extensive search of the literature has found none whose fatigue properties have been established. Although it is not directly considered in the present optimization, adequate fatigue behaviour is essential for any blade to be safe.

It is common to use a single airfoil for small blades as the large-blade practice of increasing the airfoil thickness near the root will cause undesirable aerodynamic behaviour at the low chord Reynolds number, *Re*, encountered by small blades (e.g. Wood 2011). The first airfoil considered here is the SG6043 developed for small wind turbines by Giguere and Selig (1998). As seen in Figure 1, this airfoil has an outstanding lift to drag ratio which is necessary to maximize power output. The SG6043 has a maximum thickness of 10% which may cause high stress levels near the root, so the 14% thick SD7062 (Giguere and Selig 1997) was also considered. Figure 1 shows that it has a good lift to drag ratio but is likely to produce less power than the SG6043. The noise analysis is that used by Clifton-Smith (2010) which was based on the semi-empirical formulation of Zhu et al. (2005). This objective function will not be described in detail as it is not used in this study.

One of the prime requirements for multi-dimensional optimization involving the evaluation of thousands of objective functions is their rapid evaluation. Therefore, it is not possible to use, say, detailed computational fluid dynamics or finite element structural analysis. The optimization results from SWRDC cannot be considered as final designs until validated or modified by higher-fidelity simulations. It is also necessary to emphasize that the optimization is of the aerodynamic part of the blade and excludes the structurally important connection to the turbine hub. This 'attachment section' typically does not contribute substantially to the blade inertia but is likely to carry the major blade load, the root bending moment. The assumption of hollow blades may also be a significant simplification. Some small blades use a foam core to separate the blade surfaces and prevent buckling (e.g. Clausen et al. 2013), and it is also possible for small blades to have a shear web or spar as do large blades. These additional structural features are not considered here.

The next section demonstrates the importance of starting and describes its aerodynamic modelling using a modified blade element analysis. This is followed by a description of the structural analysis. Power extraction uses standard blade element theory (e.g. Hansen 2008,

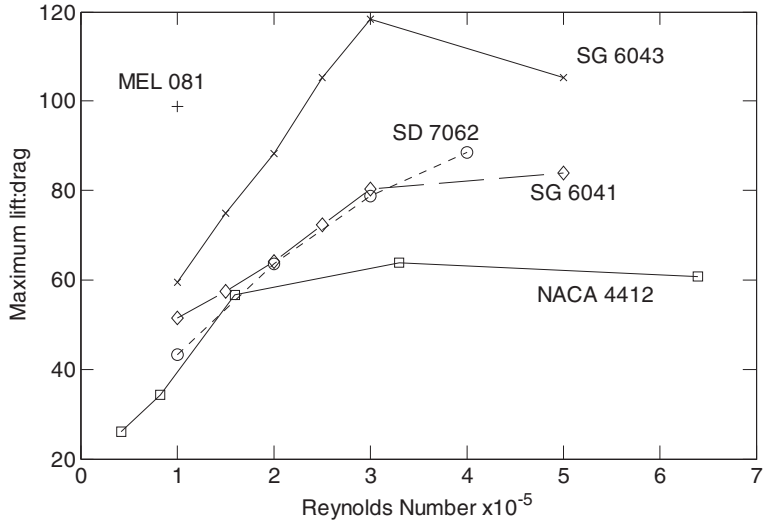

Figure 1 Airfoil lift to drag ratio at low Reynolds number from Wood (2011).

Wood 2011, and Sessarego 2013). The last reference described the detailed validation of the code in reference to the NREL code Wt_Perf using the AWT-27 turbine performance data (Buhl 2012).

Methods

Starting performance and starting time

Figure 2a shows a high-speed starting sequence of the two-bladed 5-m-diameter 5-kW wind turbine at the University of Newcastle, Australia, depicted in Figure 2b. The blades were designed by the second author for good starting performance using the analysis that is described below. Starting is important for small turbine blades which have no pitch adjustment as the stationary or slowly rotating blades experience high angles of attack, α, which generate low aerodynamic torque and lead to long starting times in which no power is extracted. Figure 2a indicates that the starting time, T_s, to reach power-extracting angular velocity is about 13 s. Since T_s scales as the inverse of the wind speed, this well-designed turbine takes around 40 s to start at a desirable cut-in wind speed of 3.5 m/s.

By assuming that starting is quasi-steady and using the generic flat plate equations for high angle lift and drag, Wood (2011) determined the aerodynamic torque, Q, for a turbine with N blades of tip radius R, generated by a wind speed U as

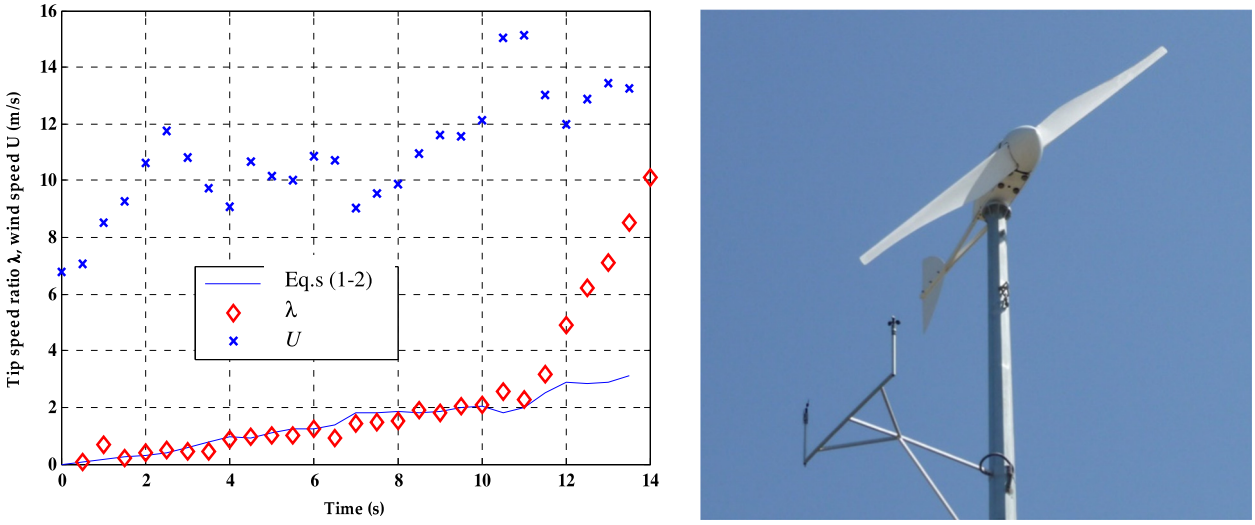

Figure 2 High-speed starting sequence of the two-bladed 5-m-diameter 5-kW wind turbine. **(a)** Measured and calculated starting performance of the 5-kW turbine shown in **(b)**.

$$Q = N\rho U^2 R^3 \int_{r_h}^{1} \left(1+\lambda_r^2\right)^{1/2} cr \sin\theta_p \left(\cos\theta_p - \lambda_r \sin\theta_p\right) dr \quad (1)$$

ρ is the air density, r_h is the normalized hub radius, and λ_r is the local speed ratio, which is the product of, r, the radius normalized by R, and λ, the tip speed ratio. Θ_p is the blade twist angle, measured from the plane of rotation. If the resistive torque of the drivetrain and generator is Q_r, then the tip speed ratio, λ, obeys

$$\frac{d\lambda}{dt} = \frac{R(Q-Q_r)}{JU} \quad (2)$$

where J is the rotor inertia. For turbines of all sizes, J is dominated by the blade inertia, J_B (Wood 2011), so that $J \sim NJ_B$. If Q_r can be neglected, as in the example shown in Figure 2, then starting becomes independent of the number of blades. Figure 2a shows the solution of Equations 1 and 2 obtained using the Adams-Moulton method and the measured U. The equations are a good fit to the measurements for the period of slow acceleration, up to around 11 s, that dominates the starting sequence. Soon after that point, the angles of attack have reduced significantly and the rotor accelerates rapidly. In general, Q_r cannot be neglected, unless it is less than about 1% of the rated torque (Wood 2011). An example of its importance is the analysis of altitude effects on small-turbine performance by Pourajjabian et al. (2014). The reduction in air density with altitude can require significant blade redesign to achieve rapid starting as the altitude increases if Q_r is not affected by altitude. Q_r is assumed to be zero for the present calculations. SWRDC solves Equations 1 and 2 for a user-specified number of blade elements; this was 30 for the present calculations. The same number of identical elements is used to find the power output.

Structural analysis

Even though the blade surface shape is determined largely by aerodynamic requirements, the structure is very important. The chosen blade materials must be sufficiently strong and resistant to fatigue, and the resulting blade inertia is a key element of the starting performance. This interaction of material properties and aerodynamics is unique to small blades and is one reason to include structural analysis in the optimization. The structural model is based on simple Euler-Bernoulli beam theory (e.g. Hansen 2008) and is a simpler version of the one used for large-blade optimization by Sessarego (2013) and Sessarego et al. (2014). They assumed a lay-up consisting of multiple laminate shells, two shear webs, fore and aft panels, and two spar caps of equal thickness. Since small turbine blades often are shells of thickness, s (Clausen et al. 2013), the structural model is shown in Figure 3. SWRDC assumes s is constant for each blade element but can vary between elements. A minimum value of s/c is a necessary user input. Actual wind turbine blades are made from composite anisotropic materials, and classical laminate theory or finite-element-based approaches must be used to predict accurately the blade structural performance (e.g. Chen et al. 2010 and Lin et al. 2010). For the current study, the complexity of the structural analysis is reduced by treating all materials as isotropic using the material properties listed in Table 1. These materials range from conventional E-glass/polyester through sustainable materials to rapid prototyping plastic. In all cases, the first two material properties were taken directly from the reference. The maximum allowable strain which must be an input to SWDRC was calculated as follows, using E-glass/polyester as an example. Table 2 of Shah et al. (2013) gives the composite strength as 567 MPa. We assume that this is the ultimate tensile strength (UTS) as is assumed for all other materials. Taking a generous 'safety factor' of 2 between the UTS and yield strength gives the latter as 283.5 MPa. The resulting maximum strain is found from Hooke's law: $283.5 \times 10^6 = 36.9 \times 10^9 \varepsilon$, where ε is the strain. Thus, ε = 7,684 μstrain. Table 2 of Shah et al. (2013) gives the composite fibre failure strain as 1.9% which is greater than 7,684 μstrain = 0.77%, so the latter value is used.

The strain is determined around the contour of the cross-section of each blade element in SWRDC to find the maximum value. The blade can be solid or hollow; in the latter case, s is calculated to ensure that the allowable maximum strain is not exceeded.

Optimization

The present calculations considered only starting and power extraction. The optimization seeks to

$$\text{minimize}\left(\max\left[w\frac{1/C_p(i) - 1/C_{p,\min}}{1/C_{p,\max} - 1/C_{p,\min}},\ (1-w)\frac{T_s(i) - T_{s,\min}}{T_{s,\max} - T_{s,\min}} \right] \right) \quad (3)$$

for blade i in the current population. C_p is the conventional power coefficient at the design wind speed, taken to be 10.5 m/s. The weight w ($0 \le w \le 1$) determines the relative significance of power extraction and starting. When $w = 1$, the optimization is purely for power. T_s in seconds is the starting time required to reach a tip speed ratio at a wind speed specified by the user. Since the calculations cover only the slow part of starting as shown in Figure 2, the actual values of T_s are not significant, but the relative magnitude of them is critical.

The blade chord and twist are determined using Bézier curves with a user-specified degree number. The number

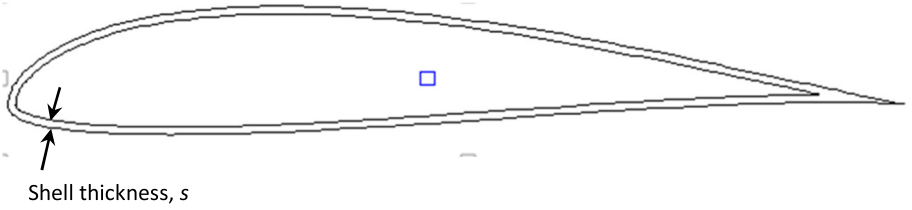

Figure 3 Structural model of a small blade.

of control points is one greater than the degree of the curves, i.e. nine control points were used for all the present calculations. Limitations on maximum and minimum chord and twist can also be specified. For all calculations, the chord was constrained between 0.04 and 0.02 m which can be viewed as realistic limitations of the manufacturing techniques. Since the minimum chord occurs at the tip, *Re* is approximately 1.7×10^5 and approximately constant along much of the blade. Similarly, the allowable twist range is 30° to −5°.

SWRDC uses a genetic algorithm (GA) for optimization, which was based on the NSGA-II C program available from the Kanpur Genetic Algorithms Laboratory[b]. The relevant inputs are entered in the Genetic Algorithm Parameters panel shown in Figure 4. A reasonable population size is needed to search the design space adequately. Numerous trials have indicated that a minimum size of 100 is necessary. This value was used in all the present calculations. The optimization stops at the maximum number of generations which was set as 100. The GA utilizes crossover and mutation operators set by the user. The crossover operator exchanges traits - the chord and twist - (called *genes*) between two or more solutions (*parents*) in the hope of producing superior solutions (*children*). Mutation ensures that each child is unique by altering their genes slightly. The crossover and mutation settings can significantly influence the performance of the GA. The Crossover Type can be either SBX or Uniform. SBX crossover is performed between two parents according to a scheme described in Deb (2001) and requires a SBX index which controls the probability of creating near-parent solutions or distant solutions as children. When Uniform is selected, a random binary vector is created and selects the genes from the first parent when the value is 1 and from the second when the value is 0, and combines the genes to form the child. The Crossover Probability controls whether the parents will be subjected to crossover or not and is a parameter for both the SBX and Uniform crossover types. The values shown in the Genetic Algorithm Parameters box in Figure 4 were used for all the present calculations.

Mutation causes small random changes to the children, promoting the diversity of the population. Only polynomial mutation as described in Deb (2001) is available in SWRDC, which depends on the Mutation Index and Mutation Probability parameters. The Mutation Index controls the intensity of the mutation (or the randomness) when altering the genes of a child. The Mutation Probability is the probability that each gene from a child will be mutated. A commonly used heuristic for Mutation Probability is 1/(number of variables) = $1/(2N + 2)$ in SWRDC, where N is the degree of the Bezier curve.

The structural analysis is combined with the aerodynamic analysis that gives the power output and starting time. For hollow blades, the shell thickness is determined by reducing the shell thickness iteratively starting from the maximum thickness value (solid blade) to the point where the specified minimum thickness (e.g. 0.01 of the chord, see subsequent paragraph) or the structural limit, defined by the maximum strain, is reached. The code gives two alternate ways of assessing structural loads, both based on the simplified load model (SLM) of the international safety standard for small turbines (International Electrotechnical Commission IEC 61400–2 ed3.0 (2013)). The SLM defines eight load cases that determine the loads mainly in the blade root and main shaft. An example of SLM analysis is given in Wood (2011) for a 0.94-m-long timber blade. It is shown that load case E 'Maximum Rotational Speed' and case H 'Parked Wind Loads' gave the greatest blade stresses. SWRDC allows the user to choose between these two cases: all the examples considered here used case H. The

Table 1 Material properties used for blade optimization

Quantity (units)	E-glass-polyester	Flax-polyester	ABS M-30	Hoop pine	Bamboo-petroleum resin
Elastic modulus (GPa)	36.9	23.4	2.4	12.1	20.5
Blade density (kg/m^3)	1,640	1,290	1,040	550	Not given
Max. strain (μstrain)	7,684	5,420	7,500	3,250	4,270

Data from Table 2 of Shah et al. (2013) (first two columns), ABS M-30 material data sheet[c], Table 1 of Peterson and Clausen (2004) for hoop pine, and Holmes et al. (2009) for the last column who gave no information on the resin.

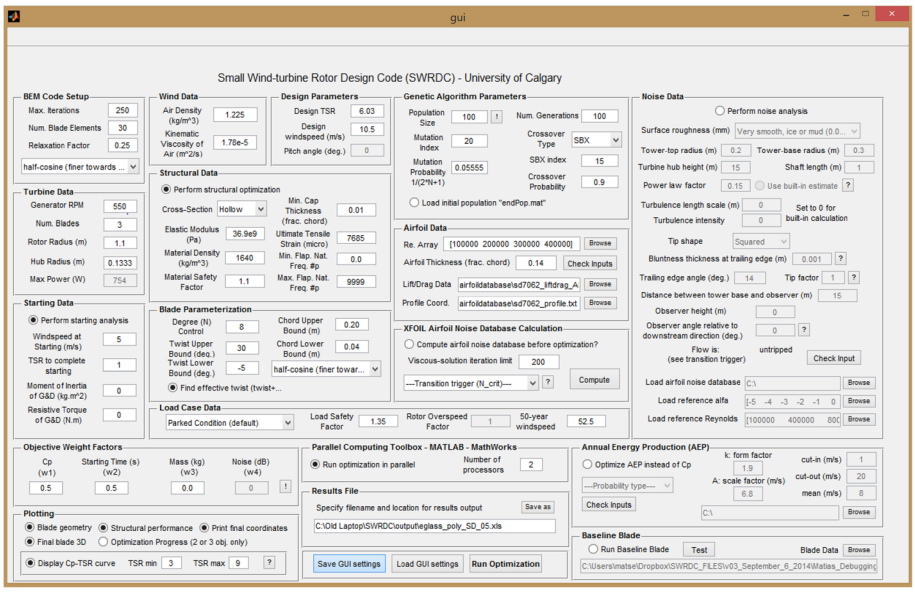

Figure 4 The Graphical User Interface of SWRDC with parameters for E-glass/polyester and $w = 0.5$.

IEC also mandates load and material safety factors. For 'full characterization' of the blade material, the material safety factor is 1.1 and the safety factor for 'aero-elastic modelling' of the loads is 1.35. This is lower than the value of 3.0 that is mandated for SLM calculations. All the present cases used an extreme (50-year) wind speed of 52.5 m/s for load case H making the design suitable for an IEC Class III wind turbine.

The three composite blades used hollow sections and the timber blade was assumed solid. The minimum shell thickness was set as 0.01 of the chord. The thickness of the blade sections shown in Clausen et al. (2013) was in the range 0.02c to 0.24c, and it is assumed that the smaller thickness is achievable. No calculations were done for the bamboo composite, whose overall performance would be similar to the flax-polyester blade.

Fatigue behaviour was not considered. The IEC SLM has only one load case (case A) for fatigue. This typically gives lower stress levels than cases E and H, but of course, the allowable stress will be much lower. According to Equation (48) of IEC 61400-2, the present blade will experience 1.73×10^{10} fatigue cycles in a 20-year life and so fatigue behaviour must be assessed very carefully. Wood (2011) showed that hoop pine has excellent fatigue properties, and it is likely that the composites studied here would also have good fatigue properties. The lack of fatigue data for ABS M-30 is a major impediment to its use for small blades.

Results and discussion

All the blade designs were found to be feasible in that the maximum strains listed in Table 1 were never exceeded in any blade. Table 2 for the SG6043 airfoil and Table 3 for the SD7062 give the power coefficient, starting time, blade mass, and the first flapwise natural frequency of the blade (see Hansen 2008) and the tip deflection for IEC load case H. As expected, the SG6043 airfoil produces more power but the approximately 2% difference is not as large as the difference in the lift to drag ratio shown in Figure 1 and may not be observable in practice. Note that for all materials, C_p and the chord and twist distributions should all be equal which is true for the thicker SD7062 (the results are not shown) but not for the SG6043 blade. The distributions in Figure 5 indicate that the ABS M-30 blade is an outlier because it needs a thicker shell: the thickness is plotted in Figure 6 for $w = 1.0$ and 0.75. In the tip region, where structural demands are low, the thickness reduces to the minimum and the chord and twist become equal to those of the other materials. For $w = 0.5$, and for all other materials at all w, the minimum $s = 0.01c$ was sufficient to ensure structural integrity.

The fundamental natural frequency should be well above the frequency corresponding to the design angular velocity of 57.6 rad/s. This is the case for all but one or two of the ABS M-30 blades. The tip deflection for IEC load case H is highest for the weakest material, ABS M-30, but in most cases is small enough to justify the use of simple beam theory which does not account for any change in shape due to the deflection.

For $w = 1$, T_s scales with blade mass as this in turn scales the inertia for constant shell thickness which results in geometrically similar blades. With decreasing w,

Table 2 Blade optimization results for the SG6043 airfoil

Material	w	C_p	T_s (s)	Mass (kg)	Frequency (rad/s)	Tip deflection (m)
E-glass/polyester	1.0	0.477	1.42	0.288	156	0.146
	0.75	0.476	1.28	0.331	175	0.231
	0.5	0.427	0.87	0.262	149	0.169
Flax/polyester	1.0	0.477	1.18	0.203	135	0.245
	0.75	0.476	1.04	0.259	146	0.202
	0.5	0.457	0.79	0.240	141	0.226
ABS M-30	1.0	0.474	1.79	0.698	81	0.447
	0.75	0.470	0.90	0.520	114	0.352
	0.5	0.464	0.84	0.523	115	0.346
Hoop pine	1.0	0.477	1.71	0.351	124	0.200
	0.75	0.475	1.54	0.516	164	0.116
	0.5	0.391	1.00	0.525	149	0.136

the general features of blade performance are common to all four materials and the two airfoils: both C_p and T_s decrease. For all materials, the decrease in C_p is significant only for $w = 0.5$: for all other w, it is unlikely that the small differences would be noticeable in terms of actual power production of a real turbine using these blades. The initial decrease in C_p with w is less than that which has been found in the previous optimizations of Wood (2011) and Pourrajabian and Mirzaei (2014). The trend in the blade mass depends on the blade material but is never monotonic.

Figures 7 and 8 show the chord and twist distributions for E-glass/polyester and ABS30 respectively. The top part of each figure gives the distributions for the SG6043 and the bottom half for the SD7062. For all materials, the changes in twist and chord are greatest near the hub, as was found by Wood (2011) and Pourrajabian and Mirzaei (2014), because the hub region generates most of the starting torque but little power-extracting torque. The E-glass/polyester chord is maximized at $w = 0.75$ for both airfoils, which gives by far the heaviest blade. The drastic change in blade shape for $w = 0.5$ is typical of these optimizations and indicates excessive emphasis on starting; for the reasons given in Wood (2011), the fastest starting blade has an infinitely small chord. In terms of the Pareto front, which should be the plot of C_p vs T_s from the optimizations, reducing w eventually increases drastically the slope of the front. Practical blades are more likely to be taken from higher values of w where reduced power extraction is more than matched by a much larger reduction in T_s. In other words, the trade-off leads to better blade designs.

For E-glass and flax blades, the better performing airfoil gave better blade designs because the minimum shell thickness was sufficient to maintain structural

Table 3 Blade optimization results for the SD7062 airfoil

Material	w	C_p	T_s (s)	Mass (kg)	Frequency (rad/s)	Tip deflection (m)
E-glass/polyester	1.0	0.468	1.67	0.482	268	0.036
	0.75	0.465	1.48	0.505	326	0.031
	0.5	0.308	0.66	0.206	142	0.205
Flax/polyester	1.0	0.469	1.36	0.386	242	0.056
	0.75	0.467	1.19	0.370	262	0.060
	0.5	0.425	0.81	0.22	201	0.129
ABS M-30	1.0	0.468	1.52	0.528	107	0.331
	0.75	0.468	1.00	0.474	131	0.274
	0.5	0.453	0.87	0.457	139	0.277
Hoop pine	1.0	0.469	2.51	0.881	207	0.038
	0.75	0.467	2.30	0.931	247	0.033
	0.5	0.410	1.44	0.549	160	0.104

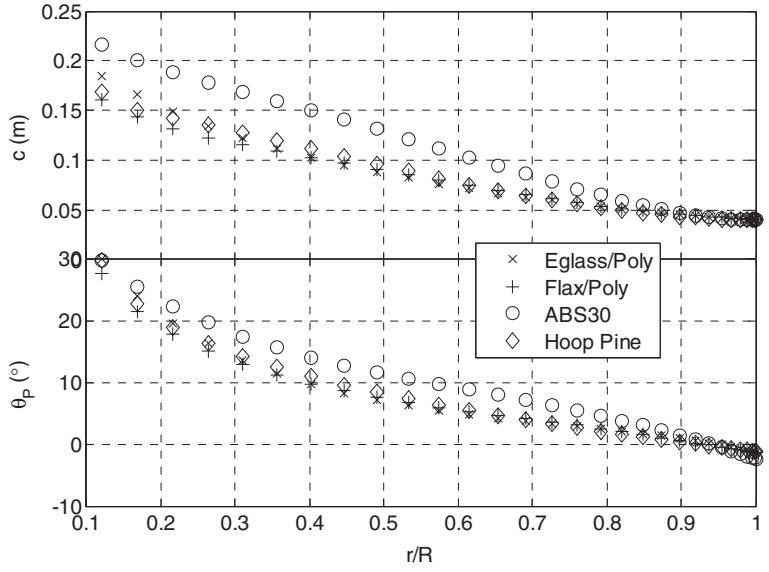

Figure 5 Optimized chord and twist for the SG6043 airfoil, ABS M-30, and $w = 1$.

integrity. This is also the case for the solid hoop pine blades which are also very strong. For ABS M-30, however, better performance was achieved with the thicker airfoil as this moved the shell further from the neutral axis and increased stiffness. A further feature of the SG6043 blades is that Θ_p near the tip is negative for $w = 1$. This is clearly needed to maximize power, but negative twist produces negative starting torque by Equation 1 and so is eliminated by the optimization process as starting becomes more important.

Conclusions

This paper describes a multi-objective optimization program for small wind turbine blade design in which the optimization can be of any combination of maximum power and minimum noise, starting time, and structure. Traditional blade element theory predicts the power extraction, and a modification of it gives the starting time. Noise is not used in the present calculations. Simple beam theory assuming isotropic material properties determines the structural strength on the basis of a choice between two load cases of the IEC 61400-2 SLM for small wind turbines. The blades are assumed hollow with a constant shell thickness. The optimization uses a GA with user input population and maximum number of generations, as well as crossover type and mutation index. Starting performance is a specific requirement of small blades that have no pitch adjustment. Since the starting time depends on the blade inertia, which in turn depends on material and density, this introduces a

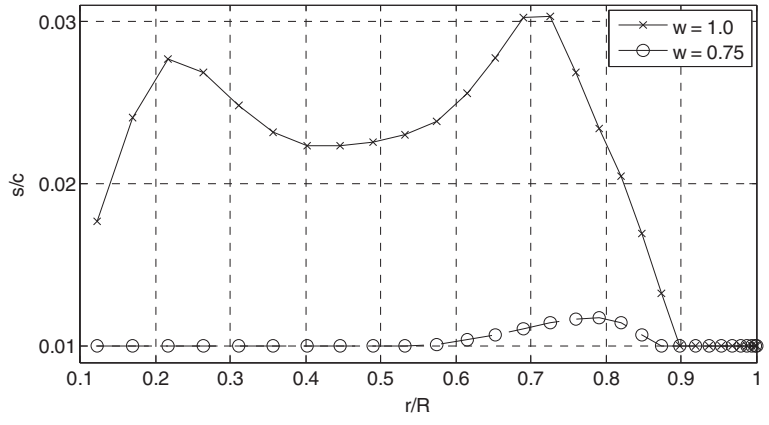

Figure 6 Shell thickness for the SG6043 airfoil and ABS M-30.

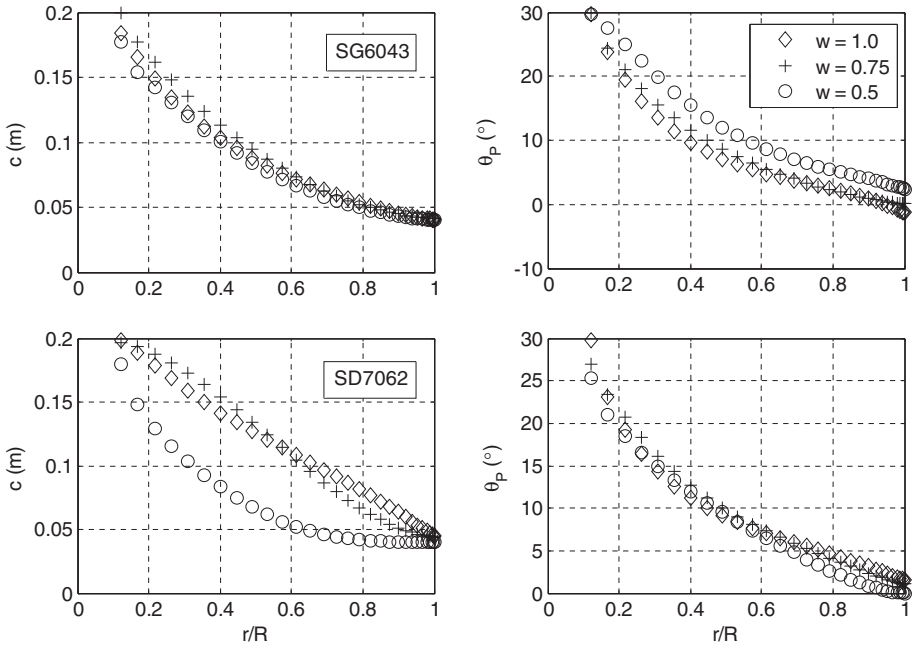

Figure 7 Optimized chord and twist for E-glass/polyester.

complex interaction between the objective functions that does not occur if design is based only on power production.

The example design is a 1.1-m blade for a permanent magnet generator producing 754 W at 550 rpm. Two airfoils are considered: the SG6043 which has the best known lift to drag ratio at Reynolds numbers typical of small turbines but is only 10% thick, and the thicker SD7062 which has 14% maximum thickness. Four blade materials were investigated:

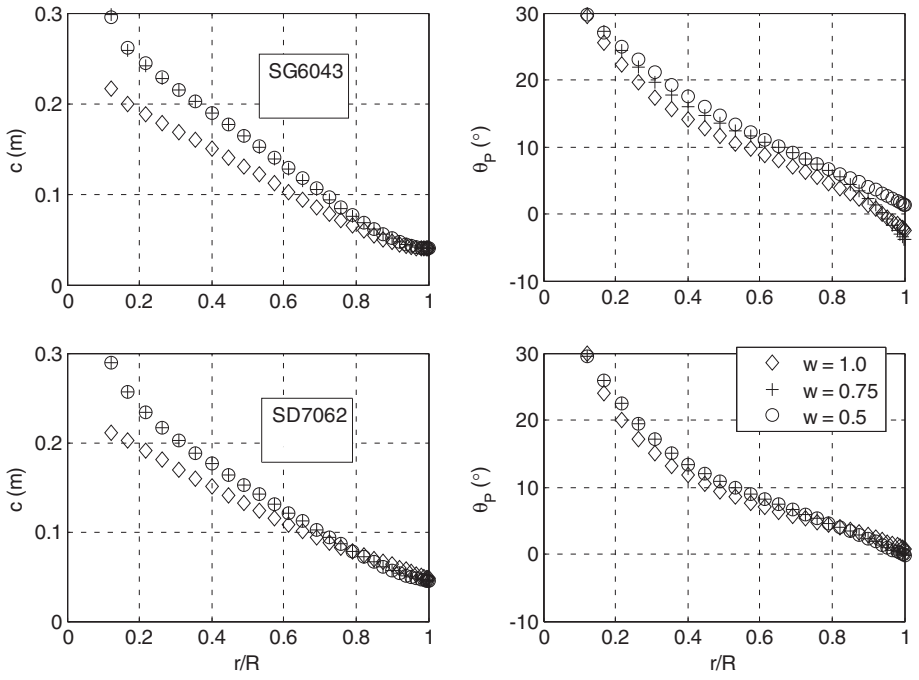

Figure 8 Optimized chord and twist for ABS M-30.

1. E-glass and polyester resin as used commonly for wind turbine blades
2. Flax and polyester, as a potential way to reduce the environmental footprint
3. A relatively strong rapid prototyping plastic
4. Timber

Optimal designs were found for power extraction only and then two cases of increasing importance of the starting time.

For materials, 1, 2, and 4, the better performing SG6043 airfoil produced slightly better power output and starting time, partly because the minimum specified shell thickness was not exceeded for any design, meaning that the materials were sufficiently strong. Generally, the chord and twist increased as more weight was given to starting. This increased the blade mass and hence the inertia, but the increase in starting torque was even greater. The changes were mostly in the hub region where more starting torque is generated, but the twist in the tip region increased from the small negative values required to maximize the power output only. This is because Equation 1 gives a negative torque for a negative twist.

It was noted that rapid prototyping has great potential for small blade manufacture as it does not require expensive moulds and can produce blades designed for specific conditions. If the technique fulfills its promise, then easily modified multi-dimensional optimization will become a routine part of the design process. Table 1 shows that the example plastic that was selected, ABS M-30, while a relatively strong plastic, is considerably weaker than materials 1, 2, and 4. It was the only material for which the shell thickness exceeded the minimum, and the thicker SD7062 airfoil was a better choice. Nevertheless, the ABS M-30 blades were not significantly inferior to the others. One crucial warning must be made about rapid prototyping: none of the materials found by the authors have been tested for fatigue which is important as the IEC 61400-2 procedure stipulates that the blades designed here will experience in excess of 10^{10} fatigue cycles over a 20-year lifetime.

The results presented here demonstrate the complex interaction between the multiple aerodynamic requirements of small wind turbine blades and the strength and density of the materials from which they are made.

Endnotes

[a]See for example, http://www.recreationalflying.com/tutorials/scratchbuilder/timber.html (accessed 13 September 2014).

[b]http://www.iitk.ac.in/kangal/codes.shtml. Version 1.1.6 was downloaded.

[c]http://www.stratasys.com/materials/fdm/abs-m30 (accessed June 6, 2015).

Competing interests
Both authors declare that they have no competing interests.

Authors' contributions
The SWRDC code was written by MS. The calculations presented here were done by DW and the paper was written jointly. The authorship is alphabetical. Both authors read and approved the final manuscript.

Acknowledgements
This research is part of a programme of work on renewable energy funded by the Natural Science and Engineering Council (NSERC) and the ENMAX Corporation. All the codes used in this paper are available without charge from the corresponding author.

Author details
[1]Department of Wind Energy, DTU, Lyngby, Denmark. [2]Department of Mechanical and Manufacturing Engineering, University of Calgary, Calgary, AB, Canada.

Received: 9 January 2015 Accepted: 30 March 2015
Published online: 01 July 2015

References

Astle, C, Burger, I, Chen, M, Herrler, T, Kwan, L, Zibin, N, et al,. (2013) Timber for Small Wind Turbine Blades. *Energy for Sustainable Development, 17*, 671–676

Adhikari, RC, Sudak, L, & Wood, DH. (2014a). Design procedure for tubular lattice towers for small wind turbines. *Wind Engineering, 38*, 359–376.

Adhikari, RC, Sudak, L, & Wood, DH. (2014b). *Bamboo for small wind turbine towers, to appear in Energy for Sustainable Development*.

Buhl, ML. (2012). *NWTC design codes: WT Perf*.

Chen, H, Yu, W, & Capellaro, M. (2010). A critical assessment of computer tools for calculating composite wind turbine blade properties. *Wind Energy, 13*(6), 497–516. doi:10.1002/we.372.

Clausen, PD, Reynal, F, & Wood, DH (2013) Design, manufacture, and testing of small wind turbine blades, Chapter 19 of *Wind Turbine Blade Design and Materials*, P. Brøndsted, P Nijssen (eds), Woodhead Publishing.

Clifton-Smith, M. (2010). Aerodynamic noise reduction for small wind turbine rotors. *Wind Engineering, 34*, 403–420.

Deb, K. (2001). *Multi-objective optimization using evolutionary algorithms*. Chichester, UK: Wiley.

Giguere, P, & Selig, MS. (1997). Low Reynolds number airfoils for small horizontal axis wind turbines. *Wind Engineering, 21*, 367–380.

Giguere, P, & Selig, MS. (1998). New airfoils for small horizontal axis wind turbines. *Journal of Solar Energy Engineering, 120*, 108–114.

Hansen, MOL. (2008). *Aerodynamics of wind turbines* (2nd ed.). London: Earthscan.

Holmes, JW, Brøndsted, P, Sørensen, BF, Jiang, Z, Sun, Z, & Chen, X. (2009). Development of a bamboo-based composite as a sustainable green material for wind turbine blades. *Wind Engineering, 33*, 197–210.

IEC 61400–2 ed3.0 (2013–12) Wind turbines. Part 2 - design requirements for small turbines.

Kaldellis, JK (ed.) (2010) Stand-alone and hybrid wind energy systems, Woodhead

Lin, H-J, Lai, W-M, & Kuo, Y-M. (2010). Combined analytical and finite element beam model for wind turbine blades. *Journal of Reinforced Plastics and Composites, 29*, 2422–2437. doi:10.1177/0731684409352386.

Peterson, P, & Clausen, PD. (2004). Timber for high efficiency small wind turbine blades. *Wind Engineering, 28*, 87–96.

Pourrajabian, A, Mirzaei, M, Ebrahimi, M, & Wood, DH. (2014). Effect of altitude on the performance of a small wind turbine blade: a case study in Iran. *Journal of Wind Engineering and Industrial Aerodynamics, 126*, 1–10.

Sessarego, M. (2013) A hybrid multi-objective evolutionary algorithm for wind-turbine blade optimization, MSc thesis, University of Calgary.

Sessarego, M, Dixon, KR, Rival, DE, & Wood, DH (2014) A hybrid multi-objective evolutionary algorithm for wind-turbine blade optimization, *Engineering Optimization* doi:10.1080/0305215X.2014.941532

Wood, DH (2011) Small wind turbines, Springer.

Shah, DU, Schubel, PJ, & Clifford, MJ. (2013). Can flax replace E-glass in structural composites? A small wind turbine blade case study. *Composites: Part B, 52*, 172–181.

Shah, H, Mathew, S, & Lim, CM. (2014). A novel low Reynolds number airfoil design for small horizontal axis wind turbines. *Wind Engineering, 38*, 377–392.

Zhu, W, Heilskov, N, Shen, W, & Sørensen, J. (2005). Modeling of aerodynamically generated noise from wind turbines. *Journal of Solar Energy Engineering, 127*, 517–528.